THE ASTROPHYSICAL JOURNAL, 402:344–357, 1993 January 1

O I LINES IN THE SUN AND STARS I. UNDERSTANDING THE RESONANCE LINES

M. CARLSSON[1] AND P. G. JUDGE[2]
Received 1992 February 7; accepted 1992 May 4

ABSTRACT

We reexamine the formation of the O I resonance lines (1302.168, 1304.858, 1306.029 Å) in chromospheric models of the Sun and cool stars. We focus on testing excitation mechanisms and understanding the dependence of the emergent spectra on the thermodynamical conditions in chromospheres.

Based upon a complete reevaluation of atomic parameters and a sensitivity analysis, we confirm the dominance of the H Lyβ pumping mechanism found in earlier work, but also find important differences. In giant stars, electron collisions do not contribute significantly to the creation or destruction of resonance line photons of O I. These lines are controlled by emission through Lyβ fluorescence and by absorption in the Si I photoionization continuum. In dwarf stars, electron collisions contribute between 5% and 20% of the total line excitation.

We derive analytical approximations for the emissivity, emergent flux densities and line ratios of the resonance lines. These formulae are based on the dominance of the Lyβ mechanism and the coupling between hydrogen and oxygen number densities through strong charge transfer reactions. The emissivity of the lines is proportional to (density) instead of the (density)^2 dependence of collisionally excited lines. We derive scaling laws for the line flux densities which are broadly consistent with stellar observations. We discuss reasons for important differences between model calculations and observations, including (1) a problem with the mean number of resonance line scatterings in giant stars, and (2) the possibility that electron collisions are more important than our calculations suggest owing to inaccurate cross sections at thermal energies.

Finally, we discuss the possible applications of these lines as diagnostics of chromospheric structure. In companion papers we will discuss other lines of O I and make more detailed comparisons with observations.

Subject headings: line: formation — Sun: chromosphere — Sun: UV radiation

1. INTRODUCTION

Traditional analyses of the chromosphere of the Sun and of stars have often been based upon profiles of emission lines of abundant ions, such as the resonance lines of H I, Ca II, or Mg II (see, e.g., Linsky 1980; Avrett 1981). With notable exceptions, many spectral diagnostics of chromospheres are ultraviolet (UV) emission lines which appear in emission against a weak UV background because collisions with thermal electrons increase the line source function as a function of height through the chromosphere (e.g., Athay 1976). Examples of such "collisionally excited" lines include the Mg II *h* and *k* lines. Collisionally excited lines dominate UV spectra of the Sun and cool dwarf stars (e.g., Jordan & Linsky 1987).

Collisions with electrons are not, however, the only ways of exciting chromospheric emission lines. Following an early proposal by Bowen (1947), but apparently unaware of solar work by Nikolsky (1960, 1964), Haisch et al. (1977) demonstrated that strong UV emission near 1304 Å observed in rocket spectra of α Boo (spectral type K1 III) could be explained by emission in the resonance lines of O I ($2p^3\,3s\,^3S^o_1 \rightarrow 2p^4\,^3P_{2,1,0}$). The emission was shown to be driven by cascades through the $3s\,^3S^o$ level following photoexcitation of the $3d\,^3D^o$ term of O I by H Lyβ (Fig. 1). Subsequent work with the *IUE* satellite revealed that strong O I emission lines are common in cool stars of low gravity, and has revealed other instances of lines which are "fluoresced" by stronger lines (e.g., Jordan & Judge 1984). Skelton & Shine (1982) demonstrated the importance of this process in exciting the O I lines in the solar chromosphere, based upon *OSO 8* data. None of these earlier studies, however, could account for the strength of the O I intersystem doublet ($2p^3\,3s\,^5S^o_2 \rightarrow 2p^4\,^3P_{2,1}$) at 1355.598, 1358.513 Å.

Many observations of the resonance lines of O I have been published. Stellar data have been acquired by several groups using *IUE* both at low dispersion (e.g., Ayres, Marstad, & Linsky 1981; Oranje 1986), and high dispersion (e.g., Brown et al. 1984; Hartmann & Avrett 1984; Ayres et al. 1986a; Judge 1986a, b). High quality solar data are available from the NRL SO-82B spectrograph aboard *Skylab* (Doschek et al. 1976; Roussel-Dupré 1985; Cappelli et al. 1989) and from NRL's high spatial resolution spectrograph (HRTS) (e.g., Athay & Dere 1991). With the aim of understanding better the nature of chromospheres of the Sun and stars using these and future observations, we have undertaken a study of the formation of O I lines. Our motivations are driven by the following:

1. After hydrogen and helium, oxygen is the most abundant element in chemically normal stars. Yet, the chromospheric spectrum of oxygen (exclusively O I) has barely been exploited in understanding chromospheric phenomena.
2. We do not know whether the H Lyβ fluorescence mechanism is responsible for O I $\lambda\lambda$1302.168, 1304.858, 1306.029 emission

[1] Institute of Theoretical Astrophysics, University of Oslo, P.O. Box 1029 Blindern, N-0315 Oslo 3, Norway.
[2] High Altitude Observatory, National Center for Atmospheric Research, P.O. Box 3000, Boulder, CO 80307. The National Center for Atmospheric Research is sponsored by the National Science Foundation.

from cool stars in general. In spite of the work of Haisch et al. (1977) and Skelton & Shine (1982), recent authors have assumed collisional control of the resonance lines of O I in their interpretation of solar data (Athay & Dere 1991).

3. Photoexcited lines provide a complementary diagnostic to collisionally excited lines, because the emergent line flux densities depend differently upon chromospheric conditions. The primary source of line photons depends linearly on a radiation field which is controlled nonlocally for photoexcited lines, and on the local electron density n_e for collisionally excited lines.

4. The observed behavior of the O I resonance line flux densities as a function of stellar chromospheric activity and gravity (e.g., Ayres, Marstad, & Linsky 1981; Oranje 1986; Cappelli et al. 1989) is not yet understood. Specifically, why are the "flux-flux relations" between the O I and collisionally excited lines essentially linear? How do the O I resonance line flux densities behave in regions of different chromospheric activity on the Sun? What do these tell us about the nature of the chromosphere in these regions?

5. New atomic data are available of higher quality than used in previous studies. How are the conclusions of earlier work affected by using updated and more complete atomic data, and an improved treatment of the radiative transfer?

6. What specific diagnostic value are the O I lines in the Sun and cool stars? What kind of modifications to chromospheric models based upon collisionally excited lines can be inferred from the photoexcited lines?

7. Presently there is much debate concerning the inhomogeneous nature of the solar chromosphere (Ayres 1981; Ayres & Testerman 1981; Ayres, Testerman, & Brault 1986; Athay & Dere 1990). How can the photoexcited lines be used to probe the inhomogeneities?

In this first paper we address the O I lines in terms of their use as spectral diagnostics of conditions in the chromospheres, focusing on the resonance lines. We identify the important processes influencing these lines and attempt to understand the detailed transfer calculations in terms of simpler, analytical models. In later papers we will study the intersystem lines at 1355.598, 1358.513 Å (Paper II) and make more detailed comparisons of the theoretical calculations and approximations with observations of the Sun and stars.

In § 2 and the Appendix we present our atomic model. In § 3 we discuss the solution of the coupled equations of radiative transfer and statistical equilibrium in available model chromospheres. In § 4 we present the results of these calculations and illustrate how the chromospheric lines respond to changes in uncertain atomic parameters. In § 5 we show how the O I line flux densities depend simply and sensitively on the radiative transfer solution for hydrogen, and derive approximate analytical formulae for the O I line flux densities in terms of the hydrogen number densities. In § 6 we briefly compare our results with previous studies and with observations, and discuss the use of the O I resonance lines as chromospheric diagnostics.

2. ATOMIC DATA

A substantial fraction of our effort was devoted to examining atomic processes influencing the UV lines of O I and in deriving a useful atomic model. Based upon a much larger model atom (to be discussed in Paper II), we found that a 14 level atom is required to account properly for the important processes influencing the resonance lines. Tables 1A & 1B lists the atomic parameters which we have adopted and Figure 1 shows the term diagram, including the radiative transitions. These parameters are discussed in the Appendix. There are some important differences between our atomic parameters and those of earlier workers:

1. We include all levels up to the $2p^3\,3d\,^3D^o$ term, in order to include important bound-bound (b–b) and bound-free (b–f) processes. Haisch et al. (1977) ignored the $2p^3\,3d\,^5D^o$ term which can contribute to the emissivity of the intersystem UV lines following recombination and radiative cascades. Skelton & Shine (1982) treated just the singlet and triplet systems except for the $2p^3\,3s\,^5S^o_2$ level, i.e., the upper level of the intersystem UV lines.

TABLE 1A

ATOMIC PARAMETERS FOR O[a]

Level	Energy (cm^{-1})	Designation
1.....	0.000	O I $2p^4\,^3P_2$
2.....	158.290	O I $2p^4\,^3P_1$
3.....	226.990	O I $2p^4\,^3P_0$
4.....	15867.862	O I $2p^4\,^1D_2$
5.....	33792.583	O I $2p^4\,^1S_0$
6.....	73768.200	O I $2p^3\,3s\,^5S^o_2$
7.....	76794.978	O I $2p^3\,3s\,^3S^o_1$
8.....	86626.910	O I $2p^3\,3p\,^5P$
9.....	88630.990	O I $2p^3\,3p\,^3P$
10.....	95476.740	O I $2p^3\,4s\,^5S^o_2$
11.....	96225.049	O I $2p^3\,4s\,^3S^o_1$
12.....	97420.758	O I $2p^3\,3d\,^5D^o$
13.....	97488.488	O I $2p^3\,3d\,^3D^o$
14.....	109837.020	O II ($^4S^o$) ground

[a] Abundance [O/H] = 8.92; atomic weight = 15.87.

TABLE 1B

b–b TRANSITIONS COMPUTED IN DETAIL

Upper j	Lower i	λ_{ji} (Å)	f_{ij}	A_{ji} (s^{-1})
6	1	1355.60	1.21(−6)[a]	4.38(3)
6	2	1358.51	6.18(−7)	1.34(3)
7	1	1302.17	5.04(−2)	3.30(8)
7	2	1304.86	5.11(−2)	2.00(8)
7	3	1306.03	5.07(−2)	6.60(7)
7	4	1641.31	2.20(−8)	9.08(1)
8	6	7774.69	9.78(−1)	3.60(7)
9	7	8446.47	1.05(0)	3.27(7)
10	8	11296.55	1.64(−1)	2.57(7)
11	1	1039.23	1.85(−3)	1.90(7)
11	2	1040.94	1.85(−3)	1.14(7)
11	3	1041.69	1.86(−3)	3.80(6)
11	9	13164.58	1.63(−1)	1.88(7)
12	8	9261.99	9.12(−1)	4.25(7)
13	1	1025.76	2.00(−2)	4.21(7)[b]
13	2	1027.43	2.00(−2)	2.53(7)
13	3	1028.16	2.00(−2)	8.41(6)
13	9	11286.77	2.69(−1)	8.45(6)

[a] $1.21(-6) \equiv 1.21 \times 10^{-6}$.

[b] This line was treated using the values of J_ν computed from the hydrogen solutions.

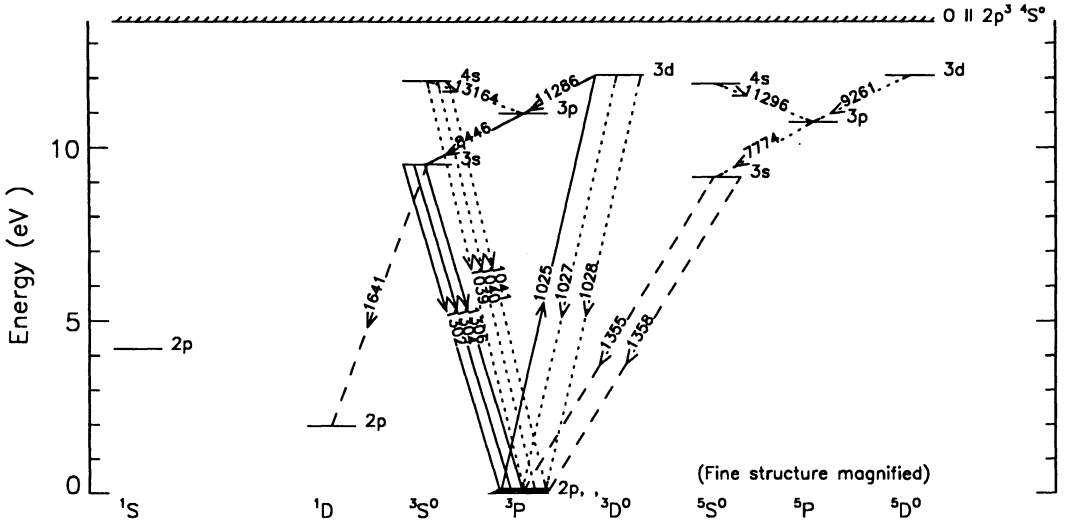

FIG. 1.—Term diagram of O I showing the levels and transitions treated explicitly in our calculations. The model is complete up to the $^3D^o$ term excited by H Lyβ.

2. We treat all *b–b* transitions in *detail.* Skelton & Shine (1982) did not compute explicitly the cascades down from the photoexcited $2p^3\,3d\,^3D^o$ term since they adopted a fixed photoexcitation rate and adopted a branching ratio to estimate the net excitation rate of the upper levels of the resonance lines. We have found significant departures from a constant branching ratio resulting from absorption of photospheric radiation in the λ11287 multiplet ($2p^3\,3d\,^3D^o \rightarrow 2p^3\,3p\,^3P$).

3. Our oscillator strengths have been taken from the lastest available studies. The most significant difference lies in the branching ratio $\tilde{\omega}\,[A_{\lambda 11287}/(A_{\lambda 11287} + A_{\lambda 1025.762})]$, which determines the strength of H Lyβ pumping: we use $\tilde{\omega} = 0.167$, compared with 0.378 (Haisch et al. 1977) and the two values 0.38 and 0.1 used by Skelton & Shine (1982).

4. Our Maxwellian-averaged collision strengths in the $2p^4\,^3P \rightarrow 2p^3\,3s\,^3S^o$ transitions are factors of eight larger (at 6000 K) than those adopted by Haisch et al. (1977) and similar to those adopted by Skelton & Shine (1982). These are important differences since we find that electron collisions between the ground levels and the $2p^3\,3s\,^5S^o$ and $2p^3\,3s\,^3S^o$ levels play essentially no role in determining the chromospheric spectrum of O I in giant stars, and a significant role in dwarf stars. Haisch et al. (1977) adopted rates from distorted wave calculations of Sawada & Ganas (1973). Skelton & Shine (1982) adopted early experimental work by Stone & Zipf (1974), but recent work by experimental groups (Zipf & Erdman 1985; Doering & Vaughan 1986; Vaughan & Doering 1987) have lead to downward revisions of these cross sections (at energies several eV above threshold). We have adopted the smaller theoretical (close coupling) cross-sections of Rountree (1977). We believe that our collisional rates are the best currently available at near-threshold energies.

5. We make calculations with both Voigt profiles (as in the earier work) and pure Doppler profiles for the UV resonance lines. The full Voigt profiles represent the complete frequency redistribution (CRD) approximation. The Doppler profiles increase the trapping of photons in the core mimicking possible effects of partial frequency redistribution (PRD) (Milkey & Mihalas 1973).

6. We have, except for test cases described below, included no coupling between the triplet and quintet series except through radiative and collisional coupling with the ground levels and the continuum. We know of no way to compute easily these collision cross sections without resorting to elaborate atomic calculations. These spin-changing collisions involve short-range exchange processes. Skelton & Shine included no such coupling. Haisch et al. (1977) did investigate the influence of collisional coupling between the $2p^3\,3s\,^3S^o$ and $2p^3\,3s\,^5S^o$ levels assuming a collision strength of unity.

7. We have included the forbidden transition $2p^3\,3s\,^3S^o \rightarrow 2p^3(^2D^o)2p\,^1D$ at 1641.305 Å, which shares a common upper level with the resonance lines. The ratio of this line flux density with the resonance lines provides a powerful and simple diagnostic of the mean number of scatterings in the resonance lines (cf. Brown, Ferraz, & Jordan 1980; Judge 1986a).

3. RADIATIVE TRANSFER CALCULATIONS IN SOLAR AND STELLAR MODEL CHROMOSPHERES

We have made non–LTE radiative transfer calculations for models of the Sun and dwarf and giant stars available in the literature. Here we discuss models of different activity on the Sun (Vernazza, Avrett, & Loeser 1981, hereafter VAL), the model of the active dwarf ϵ Eri (K2 V) (Simon, Kelch, & Linsky 1980), models of β Gem (K0 III) and α Tau (K5 III) (Kelch et al. 1978) and the model of α Boo (K1 III) of Ayres & Linsky (1975). We will focus upon α Boo and VAL model "C" as examples of the O I line formation in typical dwarf and giant stars. These models are all "thermal": the electron energy distributions are all assumed to be Boltzmann at the local electron temperature.

We used the program MULTI (Carlsson 1986), updated with an improved treatment of "background" opacities, including the formation of molecules in the number density calculations, based upon the program described by Gustafsson (1973). In the photospheres and low chromospheres of the models considered here, the partial pressures of molecules such as CO can exceed those of the individual atomic species. Molecular opacities were not included.

We solved first hydrogen and used the mean intensities in the Lyman-β line and the number densities of hydrogen for the oxygen calculations. We used the same O I atomic model for each star.

TABLE 2

RADIATION TEMPERATURES FOR HYDROGEN CONTINUA

STAR	LOWER LEVEL RADIATION TEMPERATURE (K) 2	3	4	5	SOURCE[a]
ϵ Eri	3340	3395	3465	3595	b
VAL 3F	4940	4810	4716	4738	a
VAL 3C	4940	4810	4716	4738	a
VAL 3A	4940	4810	4716	4738	a
β Gem	3942	3995	4064	4191	c
α Boo	3340	3395	3465	3595	b
α Tau	2847	2904	2978	3114	c

[a] Sources: (a) Vernazza, Avrett & Loeser 1981; (b) Ayres 1975, for ϵ Eri identical radiation temperatures to α Boo were adopted; (c) scaled linearly from the Ayres 1975 radiation temperatures for α Boo using the temperature minimum and effective temperatures ($T_R = T_{min} + f \times (T_{eff} - T_{min})$, $f = (T_R - T_{min})/(T_{eff} - T_{min})$ evaluated for α Boo.)

3.1. *Hydrogen Solutions*

Solutions in the chromosphere, where hydrogen is not fully ionized, are very sensitive to the treatment of hydrogen line and continuum radiation transfer. We have treated a five level plus continuum model atom using the atomic data listed by VAL. The neglect of higher lying levels of hydrogen means that we underestimate the total recombination coefficient by as much as 20% (VAL, Fig. 29). However, we also underestimate the photoionization rates from these higher levels which will partially compensate the additional recombination. The Lyman continuum was calculated in detail, but the Balmer, Paschen, Bracket, and Pfund continua were treated with the radiation temperatures listed in Table 2. In the photospheres (i.e., below the temperature minima), either the values listed in Table 2 or the local gas temperature were used, whichever was the larger. The tabulated values were used in the chromospheres.

Our present version of MULTI is unable to treat the partial redistribution (PRD) problem required to compute accurate number densities of the bound levels of hydrogen. Line transfer in the coupled Lyα, Lyβ, and Hα system of lines greatly influences the number densities of these levels and hence the ionization of hydrogen, which is determined (to first order) by photoionization and radiative recombination in the Balmer, Paschen, Bracket, and Pfund continua. (The Lyman continuum is close to radiative detailed balance throughout most of the model chromospheres). We mimicked the PRD effects of the trapping of Lyman line photons in the line cores by treating these lines with Doppler broadening only assuming complete redistribution (CRD), including microturbulence. In this way we obtained an approximation for the intensities within the line cores (but not the wings) which also yield reasonably reliable estimates for the total radiative rates between the bound levels in the chromosphere (Milkey & Mihalas 1973).

During these calculations we iterated between transfer calculations and hydrostatic equilibrium integrations to ensure consistency of the atomic and electron number densities. In this way we obtained a self-consistent set of number densities and mean intensities as input to the oxygen calculations, for each star.

3.2. *Oxygen Solutions*

We calculated the pumping of O I by assuming that the O I line at 1025.762 Å does not influence the H Lyβ radiation field at λ1025.72 Å, since the O I line opacity is at least four orders of magnitude smaller than the Lyβ opacity. This approximation was shown to be valid by Munday (1990). We computed the pumping rate of the $2p^3\,3d\,^3D^o$ level by direct integration of the H Lyβ mean intensity over the O I line profile, to investigate the assumption that the mean intensity is flat over the O I profile used in earlier studies.

We also used the CRD approximation in the O I line transfer calculations but to investigate the effects of PRD, two sets of calculations were performed, one with full Voigt profiles and the other with Doppler broadening only in the resonance lines.

4. RESULTS

Figure 2 shows the computed source functions S and Planck functions B of the resonance lines in the solar model and for α Boo. Two calculations for each of the cases of Doppler and Voigt profiles are shown on each figure, one which includes the effects of the H Lyβ pumping and one which does not. Figure 3 shows the line profiles corresponding to these calculations. We note the following:

1. In both stars we confirm the earlier calculations: H Lyβ is a major source of excitation of the O I resonance lines in cool stars.
2. The influence of Lyβ is greatest in the low-density chromosphere of α Boo. In the Sun, the pumping increases the source functions by an order of magnitude in comparison with a factor of $\sim 10^2$ for α Boo.
3. The source functions are enhanced above the Planck functions in the middle chromosphere through the pumping by H Lyβ. The source functions always drop rapidly to thermalize ($S \rightarrow B$) at a column mass $m \simeq 0.1$ g cm^{-2} for a star with solar metallicity (α Boo is metal-poor, [Fe/H] = -0.56, e.g., Lambert & Ries 1981), where the Si I b–f continuum becomes optically thick and hence the photon destruction probability approaches unity. Our adopted electron collision rates are too small to influence the thermalization properties of the O I lines in the models of giant stars.
4. The ionization fractions of O I and O II are dominated by the charge transfer collisions with H II and H I, respectively.

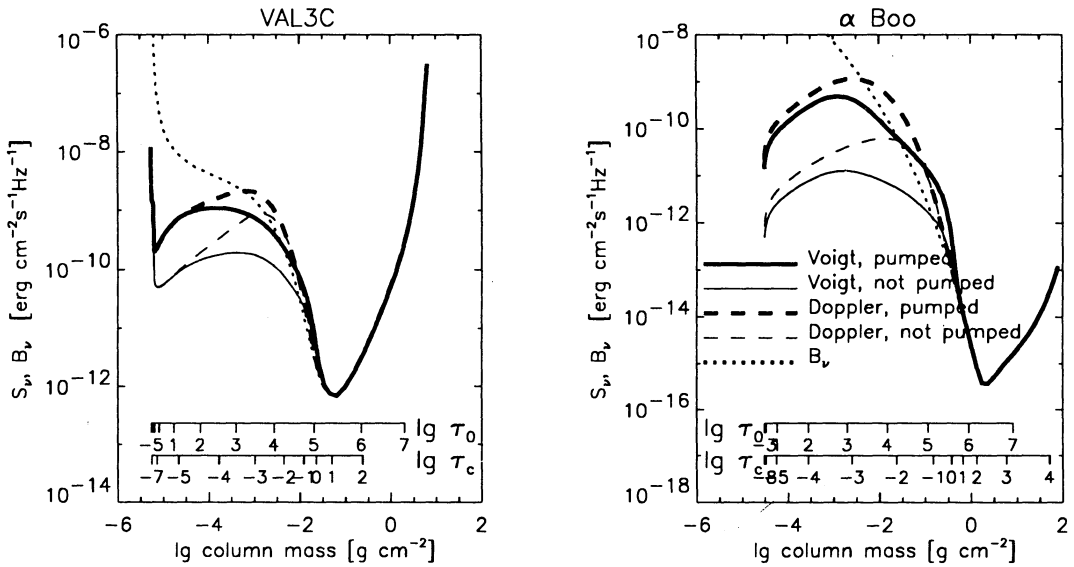

FIG. 2.—Computed source functions (*solid*, *dashed lines*) and Planck functions (*dotted line*) for the O I resonance lines in solar model C of Vernazza et al. (1981) (*left panel*) and in the model of α Boo by Ayres & Linsky (1975) (*right panel*). The different curves show source functions computed with the various assumptions described in the text. τ_c is the optical depth in the neighboring continuum, τ_0 is the optical depth at line center.

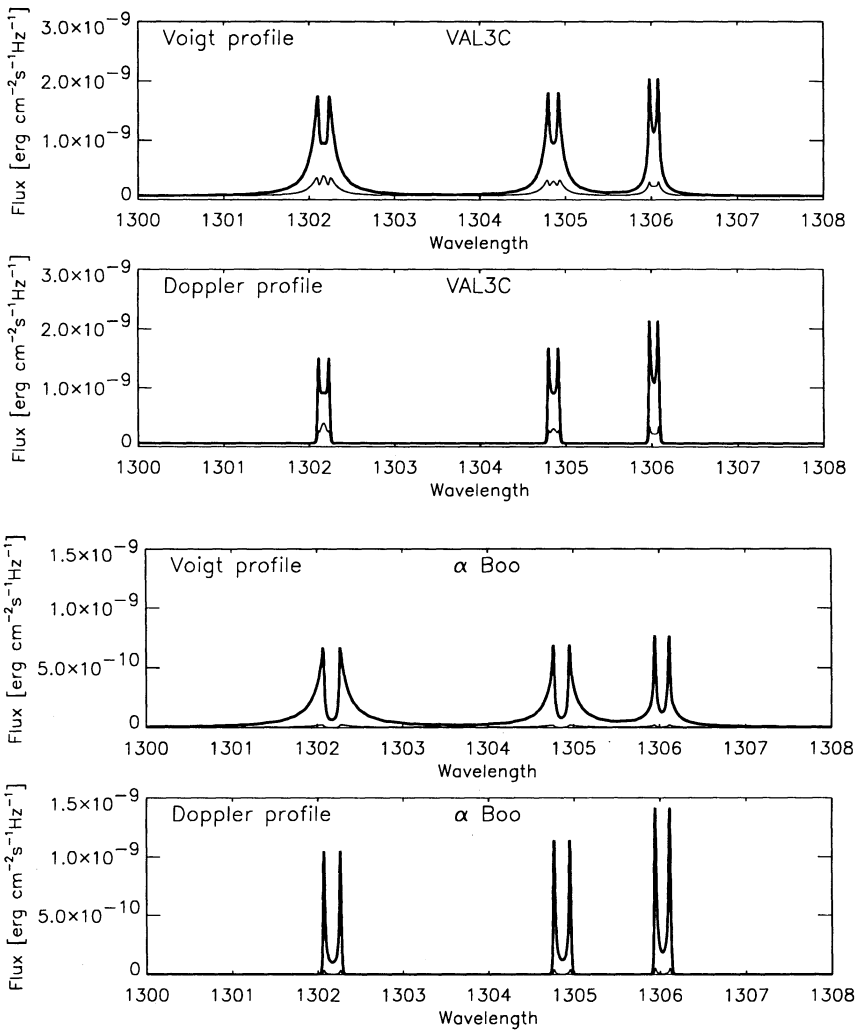

FIG. 3.—Computed line profiles corresponding to the source function calculations shown in Fig. 2

Point (3) reveals a stark difference between O I lines and collisionally excited lines (e.g., Mg II k). The Mg II lines have large collision strengths ($\Omega \sim 10$, Ω is defined below) and large collisional destruction probabilities ϵ, but small ratios of background to total opacities r (using the notation of Mihalas 1978, § 11), i.e., $\epsilon \gg r$. Exactly the opposite is true for resonance lines of O I, which have smaller collision strengths [$\Omega(\lambda 1304.858) \sim 0.03$ at 6000 K] and higher background opacities in the photoionization continuum of Si I. In our calculations, $\varepsilon \sim 5 \times 10^{-5}(n_e/10^{11})$, and $r \sim 10^{-5}$–10^{-6}. Thus, in contradiction with some previously accepted ideas (Mihalas 1978, Table 11-2), the resonance lines of O I are not controlled at all by electron collisions in giant stars ($n_e \sim 10^9$ cm^{-3} for α Boo), and are only partially controlled by collisions in dwarfs ($n_e \sim 10^{11}$–10^{12} cm^{-3} for the Sun).

Table 3 lists calculated emergent flux densities ΔF_l (ergs cm^{-2} s^{-1}), together with observations from various sources listed in the table. These are defined as the excess flux density in the line above the underlying continuum flux density F_B: $\Delta F_l = \int_{\Delta\lambda}(F_\lambda - F_B)d\lambda$, where F_B is calculated in the absence of the line. (This is related to the equivalent width w by $w = -\Delta F_l/F_B$). Three calculations for each star are listed, showing the effects of including the H Lyβ line on the O I flux densities and the effects of line transfer in the wings (Voigt profiles) versus the trapping of photons in the core (Doppler profiles).

Notice that ΔF_l(O I) are between one and three orders of magnitude larger in the giant stars than the flux densities of the lines which decay directly to the ground levels from the photoexcited state ($\lambda\lambda$1027.430, 1028.156). This may seem, at first glance, contradictory, since the branching ratio favors decays in the $\lambda\lambda$1027.430, 1028.156 transitions. The reason is that the $\lambda\lambda$1027.430, 1028.156 transitions are optically thick in the regions where the resonance lines are excited. Hence the net radiative brackets of these lines are reduced and the *effective* branching ratio for radiative decays in the λ11287 multiplet ($2p^3\,3d\,^3D^o \rightarrow 2p^3\,3p\,^3P$) is enhanced. This leads to stronger emission in the resonance lines through subsequent radiative cascades to the $2p^3\,3s\,^3S_1^o$ level (Fig. 1).

4.1. *Sensitivity of Line Flux Densities ΔF_l(O I) to Atomic Parameters*

Within MULTI we use a procedure which computes the sensitivity of line flux densities to the atomic parameters. First, solutions of the "reference" atomic model are obtained (Table 3) and the line flux densities are saved. Next, we change each atomic parameter

TABLE 3

OBSERVED AND COMPUTED LINE FLUX DENSITIES

Star	Calculation/λ [Å]	1302.168	1304.858	1306.029	1641.305	1027.430	1028.156
		Line Flux Density[$erg\ cm^{-2}\ s^{-1}$]					
ϵ Eri	Observed[a]	~5.00(3)	5.84(3)	6.81(3)			
	Voigt, Lβ	9.91(3)	8.10(3)	5.97(3)	1.13(1)	2.42(3)	1.61(3)
	Doppler, Lβ	4.12(3)	4.36(3)	4.93(3)	2.35(1)	2.42(3)	1.61(3)
	Doppler, no Lβ	5.29(2)	4.59(2)	3.72(2)	7.04(0)	-1.20(2)	-1.17(2)
VAL 3F	Voigt, Lβ	2.85(3)	2.17(3)	1.30(3)	4.38(0)	1.95(2)	1.22(2)
	Doppler, Lβ	4.29(2)	4.58(2)	5.60(2)	8.43(0)	1.95(2)	1.23(2)
	Doppler, no Lβ	7.37(1)	6.44(1)	7.02(1)	5.28(0)	-5.05(1)	-4.74(1)
VAL 3C	Observed[b]	8.74(2)	8.86(2)	1.01(3)			
	Voigt, Lβ	1.10(3)	8.59(2)	5.63(2)	1.20(0)	1.73(2)	1.13(2)
	Doppler, Lβ	2.75(2)	2.84(2)	3.24(2)	2.50(0)	1.73(2)	1.13(2)
	Doppler, no Lβ	6.44(1)	5.26(1)	4.38(1)	1.52(0)	-1.71(1)	-1.70(1)
VAL 3A	Voigt, Lβ	1.69(2)	1.30(2)	8.25(1)	2.00(1)	1.85(1)	1.07(1)
	Doppler, Lβ	3.72(1)	3.81(1)	4.47(1)	4.27(1)	1.85(1)	1.07(1)
	Doppler, no Lβ	1.10(1)	9.09(0)	9.19(0)	4.24(1)	-6.11(0)	-5.68(0)
β Gem	Observed[c]	7.91(2)	1.27(3)	1.88(3)	1.58(2)		
	Voigt, Lβ	1.73(3)	1.45(3)	1.17(3)	2.04(0)	1.18(2)	1.07(2)
	Doppler, Lβ	8.50(2)	9.33(2)	1.13(3)	3.48(0)	1.18(2)	1.07(2)
	Doppler, no Lβ	4.03(1)	3.80(1)	3.67(1)	4.74(1)	-9.33(0)	-8.90(0)
α Boo	Observed[d]	1.30(3)	1.90(3)	2.60(3)	2.90(2)		
	Voigt, Lβ	5.14(2)	3.93(2)	2.42(2)	1.03(0)	-9.17(1)	-6.78(2)
	Doppler, Lβ	1.37(2)	1.56(2)	2.02(2)	3.09(0)	-9.08(1)	-5.68(2)
	Doppler, no Lβ	3.76(0)	4.42(0)	6.17(0)	5.63(1)	-3.32(0)	-3.01(0)
α Tau	Observed[e]	7.00(2)	7.20(2)	8.00(2)	1.30(2)		
	Voigt, Lβ	1.37(3)	1.09(3)	7.79(2)	1.95(0)	3.37(1)	3.30(1)
	Doppler, Lβ	5.68(2)	6.26(2)	7.68(2)	5.70(0)	3.37(1)	3.30(1)
	Doppler, no Lβ	7.70(0)	7.11(0)	6.13(0)	3.90(2)	-5.80(1)	-6.17(1)

[a] Ayres *et al.* 1983, λ1302.168 estimated by us.
[b] Observed flux density averaged over the solar disk from scaled OSO-8 observations (Skelton & Shine 1982).
[c] Judge *et al.* 1993, in preparation.
[d] Judge 1986a.
[e] Judge 1986b.

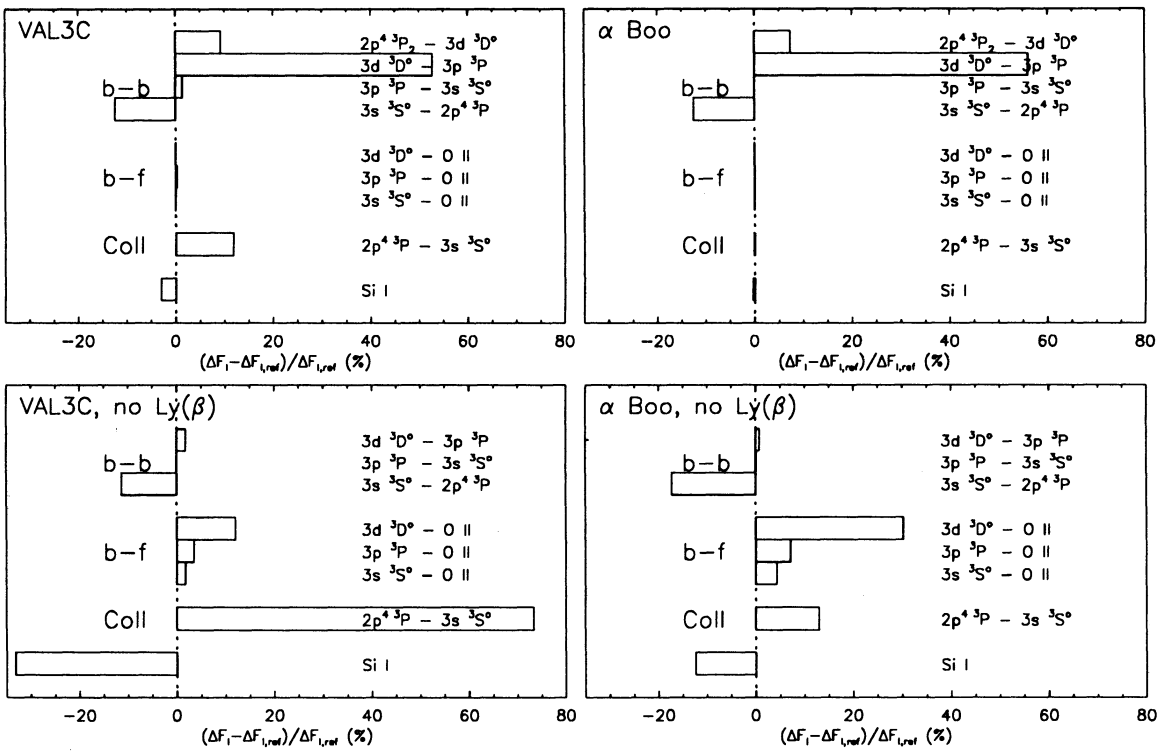

FIG. 4.—"multi-MULTI" sensitivity plot for the O I resonance lines. This graph shows the effect on the total line flux density in the resonance lines which results from doubling selected radiative bound-bound, bound-free, and collisional cross-sections and the silicon abundance one at a time. Each ordinate value represents a converged run of MULTI using the standard setup modified by doubling the indicated cross section. Plotted horizontally is the change in the computed total line flux density in the resonance lines normalized by its value in the reference setup. The cases of the Sun and α Boo are shown, both with and without the H Lyβ pumping mechanism.

keeping all others fixed by increasing the value by a factor of 2, and obtain new solutions. This is done for each oscillator strength, collision rate and photoionization cross section. Finally, for each star we obtain a matrix of values $I(j, i)$ of the percentage change in the line flux density of transition j when the parameter i is increased by a factor of 2. This arbitrary factor was selected to be big enough to reveal substantial changes but still remain close enough to a linear regime to estimate changes of the equivalent widths for other small changes of parameter i. This allows us to determine the effects of uncertain atomic parameters on our solutions and tells us what is driving the line excitation.

Figure 4 illustrates the major influences on ΔF_I of the resonance lines of O I, in the Sun and α Boo, computed using Doppler resonance line profiles, both with and without pumping. The atomic parameters which are not included in the figure have at most a 1% influence on the resonance lines in both stars. The values of ΔF_I(O I) are essentially independent of electron collision rates when H Lyβ pumping is included. Including collisions between the $2p^3\,3s\,^3S^o_1$ and $2p^3\,3s\,^5S^o_2$ levels produced changes of 2% or less in the O I resonance lines, using a "reasonable" collision strength of 2. In α Boo, the largest influence on the resonance lines comes from the oscillator strength of the λ11287 multiplet ($2p^3\,3d\,^3D^o \rightarrow 2p^3\,3p\,^3P$). Since this is the first transition in the cascade down from the $2p^3\,3d\,^3D^o$ term excited by absorption of H Lyβ photons, this confirms that the fluorescence mechanism is the dominant source of excitation of the resonance lines. In the solar case, the H Lyβ pumping rate is again the dominant source of excitation as can be seen from the substantial influence of the λ11287 and λ1025.762 ($2p^3\,3d\,^3D^o \rightarrow 2p^4\,^3P_2$) oscillator strengths.

Also shown are the effects of increasing the abundance of silicon by a factor of 2. The background opacity in the resonance lines is dominated by the Si I ($3p^2\,^3P \rightarrow$ Si II $3p\,^2P^o$) photoionization continuum, in deeper layers of the chromospheric models. Only small changes (less than a few percent) are seen by changing the Si abundance, in the pumped cases, since most of the line excitation occurs in higher layers which remain effectively thin. Larger changes are seen in the unpumped calculations, in which more of the excitation occurs in deeper layers which are effectively thick.

Comparison of the pumped and unpumped calculations in α Boo reveals that the next greatest influence on the resonance lines is the photoionization cross section from the $2p^3\,3d\,^3D^o$ level. Essentially no influence comes from electron collisions in this star. In the Sun, electron collisions play a comparable role to recombinations. We conclude that, after the Lyβ excitation process, radiative recombination is the next competing process, together with electron collisions in the high density chromospheres of dwarf stars.

5. APPROXIMATIONS

The detailed calculations reveal that chromospheric O I resonance lines are excited primarily by the absorption of H Lyβ photons followed by a radiative cascade through the resonance lines. In order to understand these calculations better, we now discuss approximations which can reproduce some essential elements of the line formation problem.

5.1. *Frequency-Integrated Flux Densities of the Resonance Lines*

We have defined the line flux density as

$$\Delta F_l \equiv \int_{\Delta\lambda} (F_\lambda - F_B) d\lambda \,, \tag{1}$$

where F_λ is the monochromatic flux density and $\Delta\lambda$ is the wavelength range covered by the resonance lines.

Since radiative cooling (or heating) is the same as the radiative flux divergence, we can write this line flux density as

$$\Delta F_l = \int_{\Delta z} (\Phi - \Phi_B) dz \equiv \int_{\Delta z} \Phi_l \, dz \,, \tag{2}$$

where Φ is the total radiative cooling over the wavelength range $\Delta\lambda$, Φ_B is the radiative cooling over the same wavelength range in the absence of lines and Φ_l is the radiative cooling in the resonance lines *defined* from this equation. Φ_l goes to zero at large depths and the integration has to be carried out over the part of the atmosphere, Δz, where Φ_l is still nonzero.

To estimate Φ_l and thus ΔF_l in the resonance line we make several assumptions:

1. Charge transfer rates of ionization and recombination are so rapid that these processes are in detailed balance (Judge 1986a). Hence

$$\frac{n(\text{O I})}{n(\text{O II})} = \frac{9}{8} \frac{n(\text{H I})}{n(\text{H II})} \,. \tag{3}$$

2. $n(\text{H I}) \gg n(\text{H II})$, (most of the emitting gas is neutral). Hence $n(\text{O I}) \gg n(\text{O II})$.

3. The $J = 0, 1, 2$ levels of the $2p^4\,{}^3P$ ground term are populated according to a Boltzmann distribution, owing to strong coupling between these levels from collisions with protons.

4. The mean intensity of H Lyβ at the frequency of the pumped O I line, $J_\nu(\text{Ly}\beta)$ is well approximated by the line source function $S_L(\text{Ly}\beta)$ with J_ν being flat across the O I λ1025.762 ($2p^3\,3d\,{}^3D^o \rightarrow 2p^4\,{}^3P_2$) absorption profile, i.e.,

$$J_\nu(\text{Ly}\beta) \simeq S_L(\text{Ly}\beta) \,. \tag{4}$$

5. The lines $\lambda\lambda$1027.430, 1028.156 are optically thick and may be approximated by assuming radiative detailed balance (i.e., the net radiative rates in these lines are much less than the rates in the cascade transitions).

6. The statistical equilibrium equation for the level $2p^3\,3d\,{}^3D^o$ is dominated by radiative rates from the level $2p^4\,{}^3P$ (upward) and by spontaneous emission to the level $2p^3\,3p\,{}^3P$ (downward). The first downward transition in the downward chain is thus assumed to have a net radiative bracket of unity.

7. The net rate in each step in the cascade chain $2p^3\,3d\,{}^3D^o \rightarrow 2p^3\,3p\,{}^3P \rightarrow 2p^3\,3s\,{}^3S^o_2 \rightarrow 2p^4\,{}^3P$ is the same as in the previous step. Hence we can express the net rate of excitation of the $2p^3\,3s\,{}^3S^o_2$ level in terms of an effective branching ratio $\tilde{\omega}$ (cf. Skelton & Shine 1982). Note that when the lines λ1027.430 and λ1028.156 are in detailed balance (item 5 above), $\tilde{\omega} = A_{\lambda 11287}/(A_{\lambda 11287} + A_{\lambda 1025.762})$ and should not be confused with the branching ratio measured by Christensen & Cunningham (1978) which is $A_{\lambda 11287}/(A_{\lambda 11287} + A_{\lambda 1025.762} + A_{\lambda 1027.430} + A_{\lambda 1028.156})$. With the atomic data listed in Table 1, $\tilde{\omega} = 0.167$.

8. The resonance lines are effectively thin in the chromosphere, i.e., all of the photons emitted in the resonance lines escape. This means that the sum of the net radiative rates from $2p^3\,3s\,{}^3S^o_2$ to levels $2p^4\,{}^3P_{2,1,0}$ is identical with $\Phi_l/h\nu$.

We will discuss the validity of these assumptions in the next subsection. The total cooling rate (ergs cm^{-3} s^{-1}) of the resonance lines using these approximations is

$$\Phi_l(\text{O I}) \simeq \tfrac{5}{9} n(\text{H I}) A(\text{O}) J_\nu(\text{Ly}\beta) B_{1\rightarrow 13} \tilde{\omega}\, h\nu_{\text{O I}} \,, \tag{5}$$

where $n(\text{H I})$ is the number density of neutral hydrogen atoms, $A(\text{O})$ is the abundance of oxygen relative to hydrogen, $B_{1\rightarrow 13}$ is the Einstein absorption coefficent for pumped transition between levels 1 ($2p^4\,{}^3P_2$) and 13 ($2p^3\,3d\,{}^3D^o$), and $h\nu_{\text{O I}}$ is the energy of a resonance line photon. In terms of the $n = 3$ hydrogen level population density $n_3(\text{H})$,

$$\Phi_l(\text{O I}) \simeq \frac{5}{81} n_3(\text{H}) \left(\frac{2h\nu^3_{\text{Ly}\beta}}{c^2} \right) A(\text{O}) B_{1\rightarrow 13} \tilde{\omega}\, h\nu_{\text{O I}} \,, \tag{6}$$

where $\nu_{\text{Ly}\beta}$ is the line frequency of Lyβ. Since the wavelengths of Lyβ and the pumped O I transition are almost identical, we can write $B_{1\rightarrow 13}(2h\nu^3_{\text{Ly}\beta}/c^2) = (g_{13}/g_1)A_{13\rightarrow 1} = (15.0/5.0)A_{13\rightarrow 1}$, then

$$\Phi_l(\text{O I}) \simeq \tfrac{5}{27} n_3(\text{H}) A(\text{O}) A_{13\rightarrow 1} \tilde{\omega}\, h\nu_{\text{O I}} \,. \tag{7}$$

With the atomic data listed in Tables 1A and 1B we have

$$\Phi_l(\text{O I}) \simeq 1.65 \times 10^{-8} n_3(\text{H}) \frac{A(\text{O})}{A(\text{O})_\odot} \,, \tag{8}$$

where $A(\text{O})_\odot$ is the oxygen abundance in the Sun (we use a value of 8.32×10^{-4}, Lambert 1978).

5.2. *Validity of Assumptions*

We have checked these assumptions against the detailed calculations. Assumptions 1–5 and 7 hold well throughout the regions of O I resonance line formation.

Assumption 6 breaks down when both the population density of the $2p^3\,3p\,{}^3P$ level and the infrared photospheric radiation

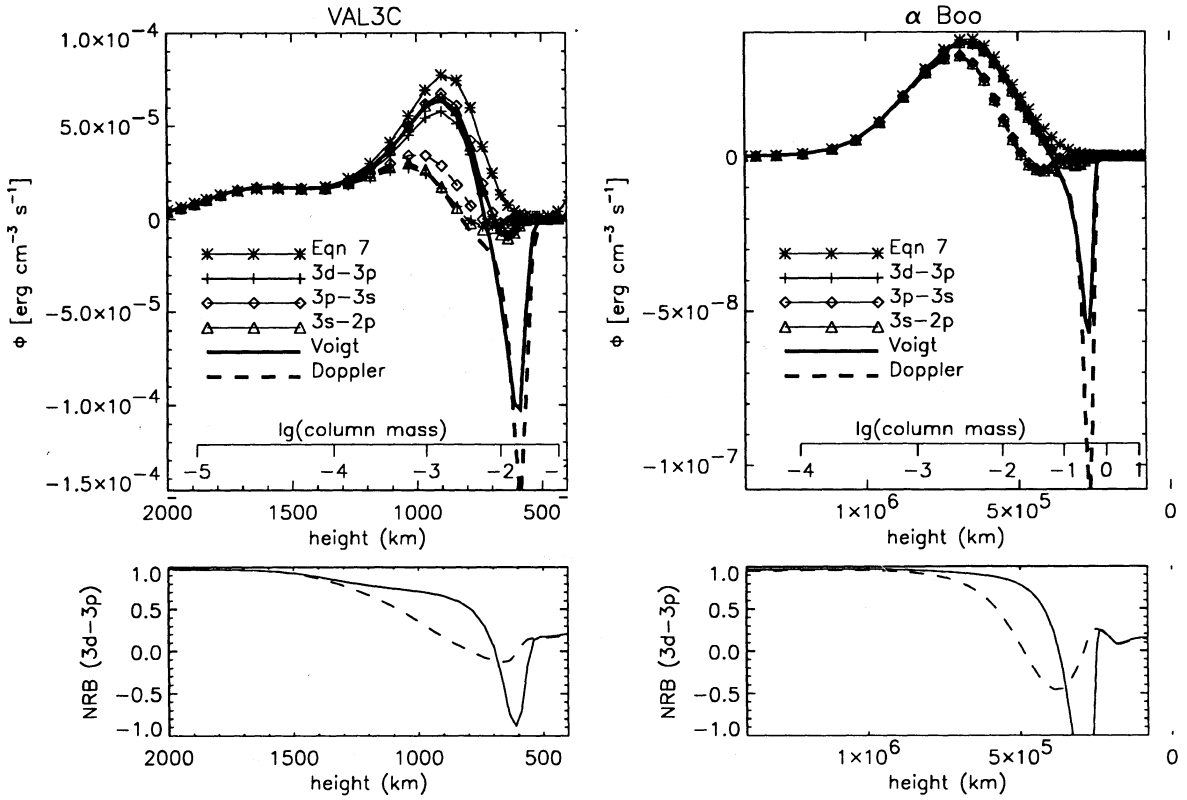

FIG. 5.—*Upper panels:* comparison of cooling rates computed in the chromospheric model "C" of VAL (*left*) and the model of α Boo of Ayres & Linsky (1975) (*right*). Solid lines show results from the computations with Voigt profiles, dashed lines show results using Doppler profiles. The thick lines show the net cooling computed from the detailed transfer equation for the three resonance lines. The thin solid line marked with asterisks (*) shows eq. (7) and other marked lines show the net radiative rates along the cascade chain. Eq. (7) differs from the cooling calculated from the net radiative rates along the cascade chain due to the neglect of absorptions in the λ11287 line ($2p^3\,3d\,^3D^o \rightarrow 2p^3\,3p\,^3P$) (see lower panels). The cooling calculated from the net radiative rates along the cascade chain differ from the net cooling due to interactions with the Si I continuum. *Lower panels*: net radiative bracket (NRB) of the transition $2p^3\,3d\,^3D^o \rightarrow 2p^3\,3p\,^3P$ (λ11287). The net radiative bracket departs from unity in the solar model at column masses between 10^{-4} and 10^{-2} g cm^{-2} owing to absorption of strong photospheric radiation in this transition. The solid line shows the net radiative bracket computed using Voigt profiles in the resonance lines, the dashed line using Doppler profiles. The difference is a result of the higher populations of the $2p^3\,3p\,^3P$ level resulting from the trapping of photons in the resonance lines in the Doppler broadened case. The effects for α Boo are substantially smaller owing to the lower radiation temperatures of a K1 star at 11287Å.

intensity are high enough that significant radiative absorption occurs in the $2p^3\,3p\,^3P \rightarrow 2p^3\,3d\,^3D^o$ (λ11287) transition. This lowers the effective branching ratio $\tilde{\omega}$, making equation (7) an overestimate of the net photoexcitation rate. It is significant for the Sun and cases with increased $2p^3\,3p\,^3P$ population density due to the trapping of resonance line photons in pure Doppler profiles. Figure 5, lower panels, shows the net radiative bracket in the λ11287 line plotted as a function of height. This is the main reason for the difference between equation (7) (*line marked with stars*, Fig. 5) and cooling rates computed from detailed calculations of the total net rates in the resonance lines (*triangles*). Note that this process invalidates the approach of Skelton & Shine (1982), who adopt a constant $\tilde{\omega}$.

Assumption 8 is invalid when the cooling rates computed from the net radiative rates in the resonance lines (lines marked with triangles) do not equal the computed radiative cooling in the resonance lines [Φ_l(O I)] (Fig. 5). This occurs when interactions with the underlying continuum become important. In the lower part of the chromosphere the lines show radiative heating due to the absorption of photons by the background continuum. This is especially true for the cases with Doppler profiles due to the lower probability of escape and thus increased probability of photon destruction in the continuum. Equation (7) again overestimates the cooling rate.

In summary, equation (7) gives a simple upper bound to the line cooling rate and hence line flux density ΔF_l(O I) in all cases studied.

5.3. *Application of Assumptions to Detailed Models*

Applying equation (7) to the models, we find that this very simple formula overestimates the detailed calculations using Voigt profiles by factors of 1.53 and 1.26 for the Sun and α Boo, respectively. This is remarkably good agreement.

The remarkable feature of equation (7) is that the O I resonance line cooling rate is directly proportional to the number density of H atoms in the $n = 3$ level. For a given chromospheric model, the $n = 3$ level population density is proportional to the proton number density, and hence also the electron number density n_e. We conclude that the O I resonance line flux densities are directly proportional to the integral of the electron density over height. These lines, excited by photons, are therefore indirect diagnostics of the chromospheric electron density.

5.4. *Comparison with Collisionally Excited Lines*

The equivalent expression for the cooling of a collisionally excited, effectively thin line such as Mg II h and k (e.g., Judge 1990) is

$$\Phi_i(\text{Mg II}) = n_i C_{ij}(T_e) h\nu_{\text{Mg II}} , \tag{9}$$

with

$$C_{ij}(T_e) = 8.63 \times 10^{-6} \frac{\Omega_{ij}}{g_i} e^{-(h\nu_{\text{Mg II}}/kT_e)} T_e^{-1/2} n_e \tag{10}$$

and Ω_{ij} is the usual Maxwellian-averaged collision strength, which for permitted lines of charged ions does not depend strongly on T_e. When $n(\text{H I}) \gg n(\text{H II})$ and $n(\text{Mg II}) \gg n(\text{Mg I})$, we obtain

$$\Phi_i(\text{Mg II}) = n_1(\text{H}) n_e A(\text{Mg}) 8.63 \times 10^{-6} \frac{\Omega_{ij}}{g_i} e^{-(h\nu_{\text{Mg II}}/kT_e)} T_e^{-1/2} h\nu_{\text{Mg II}} . \tag{11}$$

The ratio $\Phi_i(\text{O I})/\Phi_i(\text{Mg II})$ scales with the chromospheric densities and temperatures as

$$\Phi_i(\text{O I})/\Phi_i(\text{Mg II}) \propto n_3(\text{H})/[n_1(\text{H}) n_e e^{-(h\nu_{\text{Mg II}}/kT_e)} T_e^{-1/2}] . \tag{12}$$

Assuming $n_3(\text{H}) \propto n_e$, we find that the ratio of O I cooling rates to those of collisionally excited lines scales with $1/n_1(\text{H}) \propto T_e/P$, where P is the total gas pressure. This has some important consequences (see the discussion):

5.5. *Line Ratios within the Resonance Line Multiplet*

5.5.1. *Voigt Profiles*

Our calculations using Voigt profiles predict emergent line flux densities mostly in the ratios $F(1302.168):F(1304.858):F(1306.029) = 2.1:1.6:1.0$. These lines share a common upper level, and the calculations confirm that the lower levels are essentially populated according to Boltzmann statistics. Hence the line source functions of all three lines are identical at each height, but the optical depth scales differ. In the line wings the line opacity is proportional to $g_i \Gamma/x^2$ where g_i is the statistical weight of the lower level, and $x = \lambda - \lambda_0$ and λ_0 is the wavelength at line center. The damping constant Γ is dominated by radiative damping and is the same in all three lines. Thus, for a given wavelength shift in one line, x_0, we have exactly the same opacity in another line at wavelength $x_1 = \sqrt{(g_1/g_0)} x_0$. Since background opacities and Planck functions differ insignificantly between the lines we have the same opacities and the same source functions at this wavelength pair, x_0 and x_1, in the two lines and thus the same monochromatic flux density. Integrated flux densities will vary in the same way provided most of the emergent line flux density occurs at wavelengths where the damping wings dominate. Under this assumption we predict emergent flux densities of the three lines in the ratios $\sqrt{5}:\sqrt{3}:1 = 2.24:1.7:1$, values which are similar to the detailed calculations.

We conclude that most of the line transfer in our calculations using Voigt profiles is occuring in the line wings (cf. the Ayres 1979 explanation of the Wilson-Bappu effect). The small departures from these approximate ratios occur because of transfer in the core region.

5.5.2. *Doppler Profiles*

In this regime the ratios between the emergent line flux densities are "inverted", in the sense that $\Delta F_i(1302.168) < \Delta F_i(1304.858) < \Delta F_i(1306.029)$. In the optically thick limit the lines would have equal emergent flux densities. The "inverted" ratios are due to the interactions with the Si I continuum. The stronger lines undergo a larger number of scatterings and thus an increased probability of photon destruction in the background continuum. Increased number of scatterings will lead to larger inversion of the flux density ratios.

6. DISCUSSION

6.1. *A First Comparison with Observations*

The computed absolute flux densities are, with the exception of α Boo, within a factor of 2 of the observed flux densities. In these thermal models, the Lyβ mechanism is the dominant excitation mechanism of the resonance lines. We remind the reader that the chromospheric models were based upon diagnostics with quite different dependencies on the thermal structure from the O I lines.

The observed line ratios $\Delta F_i(1302.168):\Delta F_i(1304.858):\Delta F_i(1306.029)$ are all spanned by the Doppler and Voigt limits, but lying nearer to the Doppler limit in which the line ratios are "inverted". This indicates that partial redistribution is important in the formation of these line profiles. Furthermore, the computed ratios of the resonance line fluxes with the 1641.3 Å line, which shares a common upper level, reveal a related problem in our computations. In the giant stars, the resonance lines are formed too high in the atmosphere—the mean number of scatterings $\langle N \rangle$ is too small by ~two orders of magnitude. Since $\langle N \rangle \propto \tau_0$ (e.g., Frisch 1984), this implies that the mean optical depth and hence mean column mass at which the lines are formed is too small by a factor $\sim 10^2$. We discuss possible explanations for this below.

6.2. *Scaling Laws*

Ayres (1979) proposed scaling laws relating line profiles of collisionally excited emission lines to mean chromospheric properties and (through the assumption of hydrostatic equilibrium) to stellar gravities. In the spirit of Ayres's work, we can find similar scaling laws for the Lyβ-excited lines O I and compare these predictions with observations.

Ayres (1979) noted that owing to the strong temperature dependence of line cooling and the partial ionization of hydrogen, the

stellar model chromospheres are characterized by an electron density which remains nearly constant with height. This, in turn, implies that the mechanical heating rate of the chromosphere, when measured in ergs g^{-1} s^{-1} or ergs particle^{-1} s^{-1}, is roughly independent of height. This property was also noted by Avrett (1981) in the VAL solar models. If this heating is balanced by radiative losses in effectively thin collisionally excited lines, then for such a line this implies (using Mg II as an example)

$$\Phi_l(\text{Mg II})/n_1 \sim n_e \sim \text{constant} ,$$

where n_1 is the number density of the ground level of hydrogen. Comparing this with equation (7), we find

$$\frac{\Phi_l(\text{O I})}{\Phi_l(\text{Mg II})} \propto \frac{n_3}{n_1 n_e} \sim \frac{1}{n_1} .$$

Collisionally excited lines are weighted strongly towards high gas-density regions deep in the chromosphere, but the photoexcited O I lines are spread much more evenly over the chromosphere, owing to the relatively constant value of n_e in comparison with n_1. Thus, the O I lines preferentially are excited in systematically higher, less dense regions than collisionally excited lines.

We can take this kind of analysis further. From Ayres's (1979) arguments, ignoring the relatively weak dependence on effective temperature and defining $\Delta F_l(\text{TOT})$ as the total energy flux density radiated by collisionally excited chromospheric lines, Ayres's scalings for the mean chromospheric electron density $\langle n_e \rangle$ and column mass at the temperature minimum m_* can be written

$$\langle n_e \rangle \propto \sqrt{\Delta F_l(\text{TOT}) g}$$
$$m_* \propto \sqrt{\Delta F_l(\text{TOT})/g}$$

In the chromospheric models considered most of the chromospheric emission is formed within a similar number of scale heights $\Delta H \propto (T/g)$. Neglecting the small changes of temperature between chromospheric models in comparison with changes in $\Delta F_l(\text{TOT})$ and g, we can write that the total flux density of the O I lines, $\Delta F_l(\text{O I})$, should scale as

$$\Delta F_l(\text{O I}) \propto \Phi \Delta H \propto \langle n_e \rangle \frac{\langle n_3 \rangle}{\langle n_e \rangle} \Delta H ,$$

or, eliminating $\langle n_e \rangle$ in favor of $\Delta F_l(\text{TOT})$ and ΔH in favor of T/g,

$$\Delta F_l(\text{O I}) \propto \Delta F_l(\text{TOT})^{1/2} g^{-1/2} \frac{\langle n_3 \rangle}{\langle n_e \rangle} .$$

Since the total chromospheric heating, $\Delta F_l(\text{TOT})$, is controlled by collisionally excited lines, $F_l(\text{Mg II}) \propto \Delta F_l(\text{TOT})$, we get

$$\Delta F_l(\text{O I}) \propto \Delta F_l(\text{Mg II})^{1/2} g^{-1/2} \frac{\langle n_3 \rangle}{\langle n_e \rangle} .$$

Based on these dependences, the existence of tight stellar flux-flux relations (Ayres et al. 1981) and of tight relationships between the O I lines and collisionally excited lines in different regions of solar activity (Cappelli et al. 1989) implies a specific dependence of $\langle n_3 \rangle / \langle n_e \rangle$ on activity and/or gravity.

In the case of constant g (e.g., regions of varying activity on the Sun), we require $\langle n_3 \rangle / \langle n_e \rangle \sim \Delta F_l(\text{Mg II})^{1/2}$ for agreement with a linear flux-flux relationship [$\Delta F_l(\text{O I}) \propto \Delta F_l(\text{Mg II})$, as suggested by the data of Cappelli et al. 1989]. Another interesting case is that of a large variation in g. Ayres et al. (1981) found that $\Delta F_l(\text{O I}) \propto \Delta F_l(\text{Mg II})$, but with a larger constant of proportionality for giants in their sample. Combined with the solar observations this suggests that $\langle n_3 \rangle / \langle n_e \rangle$ is independent of gravity. However, the usefulness and range of applicability of these scaling laws is limited by the underlying assumptions. We consider next a breakdown of one of our earlier assumptions leading to equation (7) which could naturally explain a problem in supergiants.

6.3. *Stars of Very Low Gravity*

Recently, Carpenter et al. (1990) studied observationally the behavior of the O I resonance lines in K and M supergiant stars. They noted that $\Delta F_l(\text{O I})$ declines rapidly in comparison with collisionally excited lines, relative to less luminous giants. They were unable to identify unambiguously the cause of this behavior. Here we offer a possible solution to this problem without appealing to mechanisms outside the scope of classical non–LTE atmosphere theory.

We note that (1) the Si I photoionization continuum continues to play an important role in determining the thermalization of the O I lines [$r = \chi_c/(\chi_l + \chi_c) \sim 10^{-5}$–$10^{-6}$]; (2) our simple scaling law for $\Delta F_l(\text{O I})$ versus $\Delta F_l(\text{Mg II})$ is based upon equation (7) and therefore assumes that the O I lines are *effectively thin* in the same regions of the chromospheres; (3) collisionally excited chromospheric lines with weak background opacities (e.g., Mg II h and k) are always effectively thin in inactive cool giants and supergiants (Judge 1990). Combined with the scaling law for $m_* \propto \Delta F_l^{1/2} g^{-1/2}$, this suggests that as the gravity becomes lower, the chromospheres increase in optical depth so much that considerable fractions of the chromosphere are optically thick in the Si I continuum. For silicon fully neutral in the chromosphere, this will occur near column masses m of $10^{-2.7}$ g cm^{-2}. Furthermore, our non–LTE Si I/Si II calculations show substantially higher fractions of Si I opacity in K giants compared with dwarfs. Thus, we expect that for wavelengths below the first Si I photoionization edge (1525 Å), substantial fractions of optically thick lines will not escape from regions with $\log m > -2.7$, whereas essentially all of the Mg II emission will escape from this region.

In this picture, there is little problem in explaining the fact that the O I $\lambda\lambda$1356, 1358 lines are observed in α Ori, but the $\lambda\lambda$1302, 1304, 1306 lines are not (Hartmann & Avrett 1984). Hummer & Kunasz (1980) showed that for resonance lines embedded in a medium with a background absorber, the strongest lines are preferentially destroyed faster than the weaker lines owing to the greater path-length traveled by these photons which undergo many scatterings.

6.4. *Main-Sequence Stars and the Sun*

The observed resonance lines of O I obey reasonably tight "flux–flux correlations" with collisionally excited lines, both as a function of activity in the solar atmosphere and as a function of stellar activity amongst active stars (e.g., Cappelli et al. 1989). In short, the lines superficially behave like collisionally excited lines in these stars. As noted above, this implies a very specific behavior of the mean $n = 3$ hydrogen density n_3 and the electron density n_e in the chromosphere, *if the lines are excited by* Lyβ. However, the possibility that the lines are in reality excited by electron collisions in dwarf stars cannot be discounted if either (1) the near-threshold collision cross sections have been underestimated by factors of several by the calculations of Rountree (1977), and/or (2) the chromospheric heating mechanism leads to small populations of nonthermal electrons. Given the observational evidence, a recalculation of the collision strengths very close to threshold seems very worthwhile.

6.5. *Photoexcited Line Diagnostics in Stellar Chromospheres*

Through their dependence on nonlocally produced radiation fields and hence on integrated number densities of hydrogen, photoexcited lines of O I offer a new type of spectral diagnostic of chromospheres.

Within the context of these oversimplified models (one component, semi-infinite, plane-parallel thermal models) we find that, for a given model, the O I lines emissivities depend linearly on the electron density, and that therefore they are not as strongly weighted towards high-density (high column mass) regions of the chromosphere as the more traditional collisionally excited lines. We cannot say exactly how our conclusions will change upon relaxation of the assumptions, but we can speculate. In a highly inhomogeneous chromosphere, as envisioned by Ayres (1981), it is conceivable that "cool" regions ($T_e < T_{\rm eff}$) might radiate substantial O I fluxes owing to the transfer of Lyβ radiation emitted by hotter structures. The scales over which this might operate will depend on the scale length of transfer of "mean" Lyβ photons (i.e., the frequency-integrated kernel of the the transfer equation), and the scales of the different thermal structures. Such a phenomenon would be manifested as a "smearing" of physical structures on the solar disk seen in O I lines. This is worth further investigation. This kind of effect will also, of course, greatly influence the interpretation of all these lines from disk integrated or spatially unresolved data. It is likely that this might be intricately related to two important observations which remain in quantitative disagreement with our calculations: (1) the linearity of the "flux-flux" relations between lines of O I and Mg II, and (2) the problem of accounting for the strength of the O I λ1641.3 line in giants.

7. CONCLUSIONS

Our work represents the first systematic study of the formation of the O I resonance lines in a range of cool stars and in solar chromospheric models of various ranges of chromospheric activity. We have used totally revised estimates of atomic data and an analysis of the sensitivity of the lines to uncertain atomic parameters and approximate treatments of the radiative transfer.

We confirm that the H Lyβ pumping mechanism is the dominant source of excitation, in agreement with earlier studies. For giant stars, we find that electron collisions from the ground level have essentially no influence on these lines, which are thermalized by absorption in the Si I photoionization continuum. This has important consequences for the use of these lines as chromospheric diagnostics. In dwarf stars, a reevaluation of electron-atom collision rates between the $2p^4\,{}^3P_{2,1,0}$ and $2p^3\,3s\,{}^3S^o_1$ level at thermal energies is needed to make additional progress.

We find that the observed "inverted" line ratios cannot be reproduced by CRD calculations with Voigt profiles. Doppler profiles give the right line ratios indicating that PRD effects may be important for the formation of the resonance lines. The "inverted" line ratios and the observed λ1302/λ1641 line ratios in giants both indicate that the number of scatterings in the resonance lines is much larger than what is computed. It is speculated that this may be due to effects of inhomogeneities.

Owing to the dominance of the fluorescence mechanism, we can derive useful approximations to the line cooling rates which can be used to examine scalings of line fluxes with stellar gravity and chromospheric activity. These are in agreement with observed behavior (the flux-flux relations) only in terms of approximate scaling laws. More detailed comparisons between calculations and observations reveal some major discrepancies which we speculate are due to problems with the assumptions behind the chromospheric models themselves (notably the assumption of a homogeneous chromosphere) or perhaps with important electron-atom collision cross sections close to threshold. Nevertheless, it is clear that the O I lines will be valuable as a new type of diagnostic of the thermodynamical structure of stellar chromospheres. In future papers, we will develop an understanding of the intersystem UV lines and apply this to observations of the Sun and stars in order to understand better the nature of stellar chromospheres.

It is a pleasure to thank Peter Storey for many useful discussions and for providing the authors with subroutines which compute collisional data based upon the impact approximation. We thank Anil Pradhan for providing us with radiative data from the OPACITY project prior to publication. P. G. J. is very grateful for the award of a Fellowship from the Norwegian Research Council for Science and the Humanities (NAVF), and the High Altitude Observatory Visiting Scientists Program, which is supported by the National Science Foundation. The authors benefitted from notes on the formation of O I lines from Rob Rutten. The paper was improved by a critical reading by A. Skumanich, for which we are grateful.

APPENDIX

ATOMIC PROCESSES AND PARAMETERS FOR O I

A1. ENERGY LEVELS

Our model (Table 1) is complete up to the $2p^3\,3d\,{}^3D^o$ term. We treat all levels as real atomic levels (with energies from the compilation of Bashkin & Stoner 1975), except for levels of the $2p^3\,3p\,{}^5P$, $2p^3\,3p\,{}^3P$, $2p^3\,3d\,{}^3D^o$ and $2p^3\,3d\,{}^5D^o$ terms, whose levels are merged together into terms.

We have investigated the influence of higher lying levels on the resonance lines using a model atom with many more levels. Owing to the strength of the H Lyβ fluorescence mechanism compared with other excitation mechanisms, we have found little influence on the resonance lines from processes involving these higher levels.

Dielectronic recombination involving doubly excited states of O I can, in principle, be important at low temperatures (Storey 1981). Instead of adding more levels and transitions to account for this process we simply add the recombination rates of Nussbaumer & Storey (1986). For the case of O I we found this process to be negligible (see below).

In one calculation, we added the ground level of O III to check that we were not overestimating recombination rates from an artificially high O II population at higher chromospheric temperatures. The O III/O II ionization balance has essentially no influence on the formation of O I chromospheric lines.

A2. PHOTOIONIZATION CROSS SECTIONS AND DIELECTRONIC RECOMBINATION

Photoionization cross sections were taken from data computed by K. Butler, C. Mendoza, and C. J. Zeippen as part of the OPACITY project which is described by Seaton (1987) and Berrington et al. (1987), communicated to us by A. Pradhan. These data, computed assuming LS coupling, are known to have an accuracy of typically $\pm 10\%$. We sampled the data so that each photoionization cross section was specified at 20 wavelength points. We took care to ensure that the integrated photoionization cross sections in these sampled data were within a few percent of the original data from the OPACITY project. These calculations agree well with calculations made using identical methods but different eigenfunction basis sets by Bell et al. (1990b).

Our sampled photoionization cross sections do not contain sharp resonances responsible for the "low-temperature dielectronic recombination" (LTDR) process studied by Nussbaumer & Storey (1986). We checked the importance of these processes by adding the LTDR rates to the recombination calculation as a fixed rate using the fits given by Nussbaumer & Storey (1986), both to the ground term and to the $2p^3\,3s\,^5S^o$ term using the recombination coefficient tabulated for the λ7773.3 line. In this way we have included LTDR as an additional total recombination rate to O I and to the $2p^3\,3s\,^5S^o$ term which can potentially enhance the emissivity of the intersystem UV lines. This is equivalent to adding the higher energy levels involved in the recombination process discussed above. Since the ionization of O I is dominated entirely by charge transfer processes (see below), the photoionization cross sections and the LTDR coefficients modify just the *routes* for recombination and hence the excitation of the lines.

A3. BOUND-BOUND RADIATIVE DATA

Oscillator strengths have been taken from OPACITY project data (see above) except where reliable values of particular gf's are available in the literature. In general, the uncertainties in these data should not exceed $\pm 10\%$.

As stressed by Skelton & Shine (1982), critical oscillator strengths involve the $3d\,^3D^o$ term which is pumped by H Lyβ. The oscillator strengths of the pumped transitions ($2p^4\,^3P_{0,1,2} \rightarrow 2p^3\,3d\,^3D^o$) have been computed assuming LS coupling by varous groups. There is excellent agreement between the various calculations (OPACITY project data, Pradhan & Saraph 1977; Bell & Hibbert 1990a; Tayal & Henry 1989) and between the length and velocity forms of the radial integrals involved. Moreover, there is also excellent agreement with the value $f = 0.019 \pm 0.001$ for the measured absorption oscillator strength (Doering, Gulcicek, & Vaughan 1985). We therefore have adopted a value of 0.020 for the absorption oscillator strength.

There remains some concern over the oscillator strength of the primary cascade transition ($2p^3\,3d\,^3D^o_1 \rightarrow 2p^3\,3p\,^3P$). Recent theoretical work involving substantial basis sets for the wavefunctions all seem to yield absorption oscillator strengths $f \simeq 1$. However, this is roughly a factor of 4 greater than permitted given the branching ratio with the pumped transitions of 0.1 measured by Christensen & Cunningham (1978). This discrepancy deserves further attention owing to the importance of this oscillator strength. A possible cause of the problem might lie in the presence of a strong perturber [$(^2D^o)4s\,^3D^o$] lying between the $3d$ and $4d\,^3D^o$ terms. The substantial mixing of wavefunctions could substantially influence the oscillator strength in this transition. We have adopted an oscillator strength of 0.269 for this transition ($2p^3\,3d\,^3D^o_1 \rightarrow 2p^3\,3p\,^3P$), combining the theoretical data for the pumped transitions with the branching ratio of Christensen & Cunningham (1978).

Oscillator strengths for the UV intersystem lines ($3s\,^5S^o \rightarrow 2p^4\,^3P$) are from Zeippen, Seaton, & Morton (1977) and for the permitted transitions ($3s\,^3S^o \rightarrow 2p^4\,^3P$) are from Wiese & Martin (1980). These values are in agreement with more recent theoretical and experimental work summarized by Bell & Hibbert (1990a).

Line broadening has been computed using only radiative damping and van der Waals hydrogenic broadening estimates reliable to within a factor or 2 using the prescription of Mihalas (1978), with the coefficient $F_6 \simeq 1$. In chromospheres, densities are sufficiently low that this approximation has essentially no effect on the line profiles. Stark broadening has no influence on our computations in chromospheres owing to the dominance of van der Waals collisions and natural broadening in the largely neutral, relatively low-density chromospheric plasmas.

A4. CHARGE TRANSFER COLLISIONS WITH HYDROGEN AND PROTONS

Judge (1986a) pointed out the dominance of the charge transfer processes in stellar chromospheres following earlier work on the interstellar medium (e.g., Field & Steigman 1971; Chambaud et al. 1980). These rates are sufficiently fast that the number densities obey quite accurately the detailed balance relation: $[n(\text{O I})/n(\text{O II})] = (9/8)[n(\text{H I})/n(\text{H II})]$. (The ratio 9/8 was incorrectly inverted in Judge's discussion.) We adopted the rates of Field & Steigman (1971). These rates were computed assuming ionization from the $^3P_2$ level of O I only, appropriate for the interstellar medium. However, we require rates between the $^3P_{j=2,1,0}$ levels and the ^4S ground term of O II. We used equal ionization rate coefficients but divided the recombination rates according to the statistical weights of the lower levels.

A5. COLLISIONS WITH ELECTRONS

Ionization rates were estimated from Seaton's semi-empirical formula given by Allen (1973 § 18), similar to those used by Skelton & Shine (1982). These order-of-magnitude estimates have little effect on the calculations owing to the dominance of charge transfer ionization and radiative recombination.

Bound-bound collision rates were computed using Mendoza's (1981) compilation of collision strengths for transitions between the levels of the $3p^4$ configuration. These should be reliable to $\pm 10\%$.

Collisional rates for permitted transitions between the ground configuration and excited levels are available from a variety of sources. However, only the work of Rountree (1977) appears to address the cross sections between the $2p^4\ ^3P_{2,1,0}$ ground levels and the $2p^3\ 3s\ ^5S^o$ and $2p^3\ 3s\ ^3S^o$ levels *at near-threshold energies.* For most astrophysical applications, these low-energy cross sections are absolutely vital in determining the collision rates between the ground level and the levels of opposite parity. It is not possible to extrapolate data from higher energies for the case of electron-neutral collisions since, unlike the case of electron-ion collisions, the cross section is identically zero at threshold (Seaton 1962a). We have adopted the cross sections of Rountree, integrated over Maxwellian distributions to obtain the effective collision strengths. The accuracy of these cross sections is discussed below. We note that, at energies above ~ 4 eV above threshold, the cross sections of Rountree are in agreement (to within a factor of 2) with the more sophisticated calculations of Tayal & Henry (1988, 1989), and with recent experimental data of Gulcicek & Doering (1988).

For remaining permitted transitions we used the impact parameter approximation of Seaton (1962b), which, for permitted transitions with between relatively closely spaced levels (i.e., those above the ground configuration) should give results accurate to better than a factor of 2. These rates are a substantial improvement over semi-empirical rates or results computed using the Born approximations which overestimate collision cross sections, especially close to threshold where we require the greatest accuracy.

For other transitions we assumed (with one important exception discussed in the text) that there is no coupling between the transitions. Thus, the triplet and quintet transitions were treated in our model separately with the exception of transitions between themselves, the ground levels and the continuum $^4S^o$ level of O II. The interactions between triplet and quintet systems will be addressed in Paper II.

A6. COLLISIONS WITH PROTONS

We adopted the collision rates between the levels of the ground term compiled by Haisch et al. (1977). Other rates are negligible. These rates are sufficiently strong to force the relative populations very close to Boltzmann ratios in all our calculations.

REFERENCES

Allen, C. W. 1973, Astrophysical Quantities, 3d. ed. (London: Athlone)
Athay, R. G. 1976, The Solar Chromosphere and Corona: Quiet Sun (Dordrecht: Reidel)
Athay, R. G., & Dere, K. P. 1990, ApJ, 358, 710
———. 1991, ApJ, 379, 776
Avrett, E. H. 1981, in Solar Phenomena in Stars and Stellar Systems, ed. R. M. Bonnet & A. K. Dupree (Dordrecht: Reidel), 173
Ayres, T. R. 1975, Ph.D. thesis, Univ. Colorado
———. 1979, ApJ, 228, 509
———. 1981, ApJ, 244, 1064
Ayres, T. R., & Linsky, J. L. 1975, ApJ, 220, 660
Ayres, T. R., Linsky, J. L., Simon, T., Jordan, C., & Brown, A. 1983, ApJ, 274, 784.
Ayres, T. R., Marstad, N. C., & Linsky, J. L. 1981, ApJ, 246, 545
Ayres, T. R., Judge, P. G., Jordan, C., Brown, A., & Linsky, J. L. 1986a, ApJ, 311, 947
Ayres, T. R., & Testerman, L. 1981, ApJ, 245, 1124
Ayres, T. R., Testerman, L., & Brault, J. W. 1986, ApJ, 304, 542
Bashkin, S., & Stoner, J. O., Jr. 1975, Atomic Energy Levels and Grotrian Diagrams I. Hydrogen I–Phosphorus XV (Amsterdam: North-Holland)
Bell, K. L., Berrington, K. A., Burke, P. G., Hibbert, A., & Kingston, A. E. 1990b, J. Phys. B, 23, 2259
Bell, K. L., & Hibbert, A. 1990a, J. Phys. B, 23, 2673
Berrington, K. A., Burke, P. G., Butler, K., Seaton, M. J., Storey, P. J., Taylor, K. T., & Yu Yan, 1987, J. Phys. B, 20, 6379
Bowen, I. S. 1947, PASP, 59, 196
Brown, A., Ferraz, M., & Jordan, C. 1980, in The Universe at Ultraviolet Wavelengths: the First Two years of *IUE*, ed. R. D. Chapman (NASA CP 2171), 297
Brown, A., Jordan, C., Stencel, R. E., Linsky, J. L., & Ayres, T. R. 1984, ApJ, 283, 731
Cappelli, A., Cerruti-Sola, M., Cheng, C. C., & Pallavicini, R. 1989, A&A, 213, 226
Carlsson, M. 1986, A Program for Solving Multi-level Non–LTE Radiative Transfer Problems in Moving or Static Atmospheres (Uppsala Obs. Rept. 33)
Carpenter, K. G., Norman, D., Robinson, R. D., Fernández-Villacañas, J. L., Jordan, C., & Judge, P. G. 1990, in Evolution in Astrophysics, ed. E. Rolfe, (ESA SP-310), 307
Chambaud, G., Launay, J. M., Levy, B., Millie, P., Roueff, E., & Tran Minh, F. 1980, J. Phys. B, 13, 4205
Christensen, A. B., & Cunningham, A. J. 1978, J. Geophys. Res., 83, 4393
Doering, J. P., Gulcicek, E. E., & Vaughan, S. O. 1985, J. Geophys. Res., 90, 5279
Doering, J. P., & Vaughan, S. O. 1986, J. Geophys. Res., 91, 3279
Doschek, G., Feldman, U., Van Hoosier, M. E., & Bartoe, J. D. F. 1976, ApJS, 31, 417
Field, G. B., & Steigman, G. 1971, ApJ, 166, 59
Frisch, H. 1984, in Methods in Radiative Transfer, ed. W. Kalkofen (Cambridge: Cambridge Univ. Press), 65
Froese Fischer, C. 1987, J. Phys. B, 20, 1193
Gulcicek, E. E., & Doering, J. P. 1988, J. Geophys. Res., 93, 5879
Gustafsson, B. 1973, Uppsala Astr. Obs. Ann., Band 5, No 6
Haisch, B. M., Linsky, J. L., Weinstein, A., & Shine, R. 1977, ApJ, 214, 785
Hartmann, L., & Avrett, E. H. 1984, ApJ, 284, 238
Hummer, D. G., & Kunasz, P. B. 1980, ApJ, 236, 609
Ivanov, V. V. 1973, Transfer of Radiation on Spectral Lines, transl. D. G. Hummer (NBS Spec. Pub., No 385)
Jordan, C., & Judge, P. G. 1984, Phys. Scripta, T8, 43
Jordan, C., & Linsky, J. L. 1987, in Exploring the Universe with the *IUE* Satellite, ed. Y. Kondo (Dordrecht: Reidel), 259
Judge, P. G. 1986a, MNRAS, 221, 119
———. 1986b, MNRAS, 223, 239
———. 1990, ApJ, 348, 279
Kelch, W. L., Linsky, J. L., Basri, G. S., Chiu, H., Chang, S., Maran, S. P., & Furenlid, I. 1978, ApJ, 220, 962
Lambert, D. L. 1978, MNRAS, 182, 249
Lambert, D. L., & Ries, L. M. 1981, ApJ, 248, 228
Linsky, J. L. 1980, ARA&A, 18, 439
Mendoza, C. 1981, in Planetary Nebulae, ed. D. R. Flower (Dordrecht: Reidel), 143
Mihalas, D. 1978, Stellar Atmospheres (San Francisco: Freeman)
Milkey, R. W., & Mihalas, D. 1973, ApJ, 185, 709
Munday, M. 1990, Ph.D. thesis, Oxford Univ.
Nikolsky, J. M. 1960, Dokl. Akad. Nauk SSSR, 130, 51
———. 1964, Geomagnetism i Aeronomiyk, 4, 209
Nussbaumer, H., & Storey, P. J. 1986, A&AS, 64, 545
Oranje, B. J. 1986, A&A, 154, 185
Pradhan, A. K., & Saraph, H. E. 1977, J. Phys. B, 10, 3665
Rountree, S. P. 1977, J. Phys. B, 10, 2719
Roussel-Dupré, D. 1985, A&A, 153, 116
Sawada, T., & Ganas, P. 1973, Phys. Rev. A, 7, 617
Seaton, M. J. 1962a, in Atomic and Molecular Processes, ed. D. R. Bates (NY: Academic Press), 374
———. 1962b, Proc. Phys. Soc., 79, 1105
———. 1987, J. Phys. B, 20, 6363
Simon, T., Kelch, W., & Linsky, J. L. 1980, ApJ, 237, 72
Skelton, D. L., & Shine, R. A. 1982, ApJ, 259, 869
Stone, E. J., & Zipf, E. C. 1974, J. Chem. Phys., 60, 4237
Storey, P. J. 1981, MNRAS, 195, 27P
Tayal, S. S., & Henry, R. J. W. 1988, Phys. Rev. A., 38, 5945
———. 1989, Phys. Rev. A., 39, 4531
Vaughan, S. O., & Doering, J. P. 1987, J. Geophys. Res., 92, 7749
Vernazza, J. E., Avrett, E. H., & Loeser, R. 1981, ApJS, 45, 635 (VAL)
Wiese, W. L., & Martin, G. A. 1980, Wavelengths and Transition Probabilities for Atoms and Atomic Ions (NSRDS-NBS 68, vol. 2)
Zeippen, C. J., Seaton, M. J., & Morton, D. C. 1977, MNRAS, 181, 527
Zipf, E. C., & Erdman, P. W. 1985, J. Geophys. Res., 90, 11087